ZnO Nanoparticles Embedded in PES-LiCl-PVA Polymeric Matrix for Synthesis of Nanocomposite Hollow Fibre Membranes

Zulfida Mohamad, Hafis Mohd Shafie, Abdul Latif Ahmad*

School of Chemical Engineering, Universiti Sains Malaysia, 14300 Nibong Tebal, Penang, Malaysia
chlatif@usm.my

It is suggested that hollow fibre (HF) membranes with enhanced flux and rejection performance could be synthesised by adding zinc oxide nano particles (ZnO-NP) stabilised sterically with polyvinyl alcohol-lithium chloride (PVA-LiCl) mix into the dope solutions. Nanocomposite HF membranes made up of polyethersulfone (PES) and N,N-dimethylacetamide (DMAc) as the base components were spun out. For this study, the effect of ZnO-NP concentrations was looked into. The HF membranes were characterised using SEM and contact angle goniometry, and the performance in terms of water flux and humic acid (HA) rejection were analysed. Experimental result suggests that the ZnO-NP embedded is able to improve the water flux and HA rejection as compared to the pristine counterpart, with maximum water flux of 42.18 kg/m^2.h and HA rejection of 94.43 % when mixed at 1 and 2 wt% of ZnO-NP. In conclusion, new blends of nanocomposite HF membranes with improved flux and rejection performance were successfully formulated and synthesised.

1. Introduction

Membrane technology offers additional advantages as compared to other separation methods including high stability and efficiency, low energy requirements and ease of operation (Zhao et al., 2015). Several types of membrane housings or modules are available nowadays, namely flat sheet, spiral wound, tubular and hollow fibre (Ghosh, 2009). Hollow fibre (HF), serves several key advantages as compared to the others. Examples are higher packing densities, larger surface areas (Moch Jr., 2004), higher productivity per unit volume, self-supporting, and high recovery toleration in each individual membrane units (Kirk-Othmer, 1998). However it suffers from its manufacturing complexity (Ulbricht, 2011) and being sensitive to fouling due to lower free space between the fibres (Kirk-Othmer, 1998).

Among all of the hydrophilic modification proposed by fellow researchers to mitigate fouling issue, blending is the simplest yet effective method to be done. Modification is done during the dope preparation phase through physical mixing of membrane solution with additional hydrophilic blends, which can be polymers, nanoparticles or mixtures of both (Balta et al., 2012). It is important to note that the nanoparticle needs to be well dispersed in order to maximise the nano-gap formation (narrow gap surrounding the nanoparticles, which improves the permeability of the membrane), as agglomerated nanoparticles reduced the surface area/weight ratio (Ng et al., 2011). The possibility for the membrane pores to be blocked were also increased with nanoparticle sizes, hence further reducing the membrane's permeability below what pristine membranes could do. Nanoparticle addition is usually accompanied with polymer addition, which acts as both nanoparticle stabiliser and hydrophilic enhancer. Notwithstanding the solution proposed, nanoparticles are thermodynamically unstable in nature and will still pose its upper limit before the performance of the membranes deteriorate with increased nanoparticle concentration. It is important for researchers to study the flux and rejection of the proposed antifouling membranes as an ideally non-fouling membrane will not serve its purpose if the performances and structures are excessively become worse.

Studies by several researchers on antifouling membrane's flux and rejection performances are highlighted here. Yuan et al. (2014) have extensively studied the antifouling properties of PES ultrafiltration membrane through PVA blending in DMSO solvent, with positive result. The use of PVA as additive has also been

studied by Zhang et al. (2014) for PVDF/PES blend membrane. In this study, the membrane blends were tested in pilot scale with improved hydrophilicity and permeability at 0.3 % addition of PVA. Leo et al. (2012) have successfully synthesised PSf/PVA membranes embedded with ZnO-NP in NMP solvent for oleic acid removal. The result suggested the improvement of permeability at 2 wt% of ZnO-NP addition. Similar project has also been conducted by Zhao et al. (2015) by fabricating ultrafiltration membrane through incorporation of ZnO-DMF dispersion in PES and PVP, which improves the water fluxes by 210 % as compared to the pristine PES membrane.

In this study, the effect of nanoparticle concentration on the membrane was chosen as the parameter of interest. Preliminary studies were conducted in terms of HF membrane fabrication and the effect of embedded nanoparticles onto the structure, contact angle, flux and rejection performances. Polyethersulfone (PES) was used as the membrane matrix, while polyvinyl alcohol (PVA) and zinc oxide nanoparticles (ZnO-NP) was chosen as the main additives. Fully hydrolysed PVA are insoluble in non-aqueous medium due to extreme inter and intra molecular hydrogen bonding between its abundant hydroxyl groups (Chetri et al., 2008). This makes blending difficult as it couldn't be dissolved in many polar organic solvent, including N,N-dimethylacetamide (DMAc). Lithium chloride (LiCl) will be added to mitigate the issue. The LiCl-PVA mixture was used as the hydrophilic filler, pore former and nanoparticle stabiliser alongside DMAc solvent, which all three forms a transition state for better PVA solubility (Tosh et al., 1999). Humic acid (HA) was used as model natural organic matter (NOM) foulant for this study.

2. Methodology

2.1 Membrane Fabrication and Module Preparation

Dope solutions were prepared with increasing ZnO-NP concentrations, summarised in Table 1. PES/DMAc/PVA were maintained at weight ratio of 17.5 / 79.5 / 1.0 while LiCl was added equimolar to the amount of PVA added. All of the components were fixed in mass throughout the experiment except for ZnO-NP. LiCl was premixed in DMAc using magnetic stirrer for 30 min at 60 °C, 500 RPM. ZnO-NP was then added into the LiCl-DMAc mixture and mixed for another 15 min under the same conditions. PVA was then added into the mixture and mixed for another 3 h. The blends were then sonicated using ultrasonicator probe (Telsonic Ultrasonix SG-24-500 P) for 15 min, and then further homogenised using ultrasonicator bath (Elmasonic S80H) for another 1 h at room temperature to further improve the ZnO-NP dispersion in the solvent. Dried PES flakes were then added and mixed for 18 h at 60 °C, 700 RPM using mechanical stirrer. Once fully mixed, the dope solutions were placed back in ultrasonicator bath for degassing purpose, for another 1 h. The solutions were then ready to be used for HF membrane spinning. The synthesised dope solutions were spun at fixed spinning conditions (summarised in Table 2) through dry jet wet spinning method. Filtered water & distilled water were used as both coagulation bath & bore fluid. Spun membranes were then immersed in water for 2 d to completely remove any traces of solvent. The membranes were then immersed in 50 vol% of glycerol/water mixture for 1 d and dried under ambient conditions to preserve the membrane's pore structures. Prior to flux testing, the membranes were prepared into modules with 4 strands per module, immersed in ethanol for 6 h to remove the glycerol and kept in cold water until further usage.

Table 1: Compositions of fabricated HF membranes

Membrane Samples	ZnO-NP composition (g)	ZnO-NP composition (wt%)
A.1	0	0
A.2	4	1
A.3	8	2
A.4	12	3

Table 2: Spinning conditions of the HF membranes

Parameter	Value
Dope speed	15 RPM
Take up drum speed	8.580 RPM
Bore fluid speed	2.30 mL/min
Air gap length	15 cm
Dope pressure	1.5 bar
Spinneret diameters	OD = 1.015 ± 0.002 cm
Bore fluid outlet diameters	OD = 0.590 ± 0.002 cm; ID = 0.281 ± 0.005 cm

2.2 Membrane Morphology & Contact Angle Measurement

The HF membrane's surface and cross sectional morphologies were observed under scanning electron microscope, SEM (Hitachi TM 3000 Tabletop). Prior to the characterisation, the membrane samples were coated with thin layer of gold/palladium using sputter coater (Quorum SC7620) for 90 s. As for the cross-sectional morphology, membranes were firstly cracked by using liquid nitrogen in order to get a clean cut of the membranes. Circumference of the membranes were noted for flux calculation. Contact angle goniometry (Rame-Hart 250-U1) was also used to study the hydrophilicity of the membranes. A clean strand of HF membrane was attached horizontally to a glass plate using double sided tape and gently introduced to 2 µL of deionised water on the outer surface using a computer controlled micro syringe. The contact angle was then noted after 90 s by using DROPimage Advanced image analysis software (DROPimage, 2016).

2.3 Flux and Rejection Performance

Prior to flux performance test, the prepared membrane modules were subjected to hydraulic compression at 2 bar for 1 hour, using deionised water as the feed. The membrane modules were then tested for pure water flux (PWF) at 1.5 bar for 2 h. The flux was calculated according to the following Eq(1):

$$J = \frac{m}{4 \times C_o \times L_e \times \Delta t} \tag{1}$$

where, J (kg m^{-2} h^{-1}) is the flux, m (kg) is the mass of permeate, C_o (m) is the average outer circumference of the membrane, L_e (m) is the effective length of the membrane strands and Δt (h) is the permeation time. All flux testing was conducted at constant flowrate of 400 mL/min. To determine the rejection performance, feed solution of 60 mg/L humic acid in deionised water (adjusted to pH 7.4 using 0.1 M NaOH solution) were introduced for another 2 h at the same pressure and flowrate. Sample of permeate was taken for HA rejection determination using UV-vis spectrometer (Merck Spectroquant Pharo 300) at the wavelength of 254 nm. The rejections were calculated as in Eq(2):

$$R\,(\%) = \left(1 - \frac{C_p}{C_f}\right) \times 100\,\% \tag{2}$$

where, R (%) is the HA rejection, C_p (mg/L) is the HA concentration of permeate and C_f (mg/L) is the HA concentration of the feed.

3. Results and Discussion

3.1 Membrane's Cross Sectional and Surface Morphology
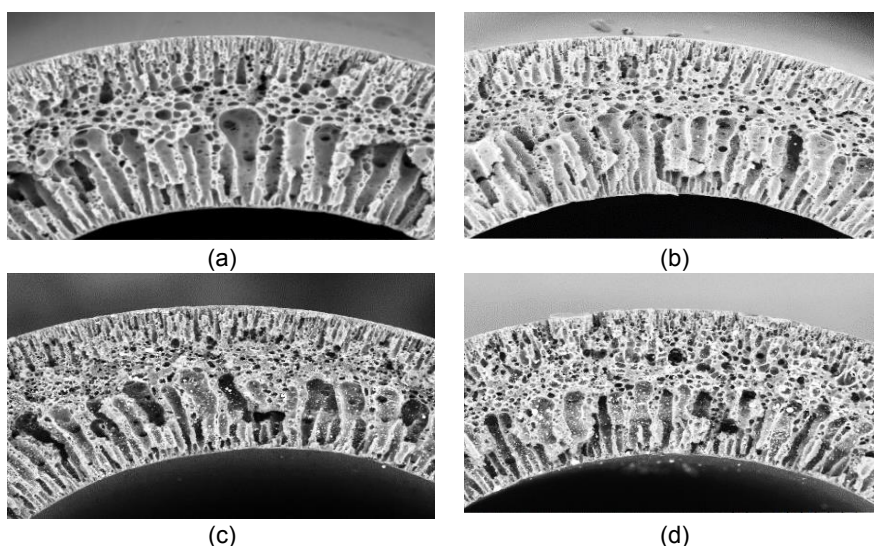

(a)	(b)
(c)	(d)

Figure 1: Cross sectional micrograph of sample (a) A.1, (b) A.2, (c) A.3 and (d) A.4 under 600x magnification

SEM observations of the cross-sectional micrograph (Figure 1) revealed the inner structure of HF membranes. Long finger like pore structures protruding from both the outer and the inner membrane surface could be seen, with irregular macro voids formed in between for all samples of membranes. Similar irregular structures had

also been noticed on PES/PVA flat sheet membranes (Yuan et al., 2014) and on PVDF/PVA hollow fibre membranes, albeit smaller in size (Li et al., 2010). This suggest that the structures are formed due to the presence of PVA. The macro voids were seen to be suppressed with increasing ZnO-NP concentration, as the finger-like structures were leaner while the irregular pores were smaller. The addition of ZnO-NP has been noted to increase the dope solution's viscosity (Ahmad et al., 2014). The increased viscosity induced a denser membrane, due to reduced solvent-nonsolvent exchange rate during the coagulation period (Guillen et al., 2011). As the demixing was delayed, macro voids were suppressed. It was also noted that the finger like structures were much longer on the inside rather than the outside for all samples of membranes. It is suggested that the finger-like structures were born from the fast phase separation (instantaneous demixing) by the bore and coagulation fluid, in which the inner pores were much larger than the outer, suggesting the effect of dry jet and air gap on suppressing the finger-like formation. The lower evaporation rate of DMAc in air compared to the demixing in the coagulation bath created a denser outer skin on the HF membranes. This is contrary to the inner lumen condition where bore fluid was in contact with the dope solution as soon as they came out of the spinneret. As a result, subsequent phase separation in the coagulation bath was faster on the inside compared to the outside of the HF.
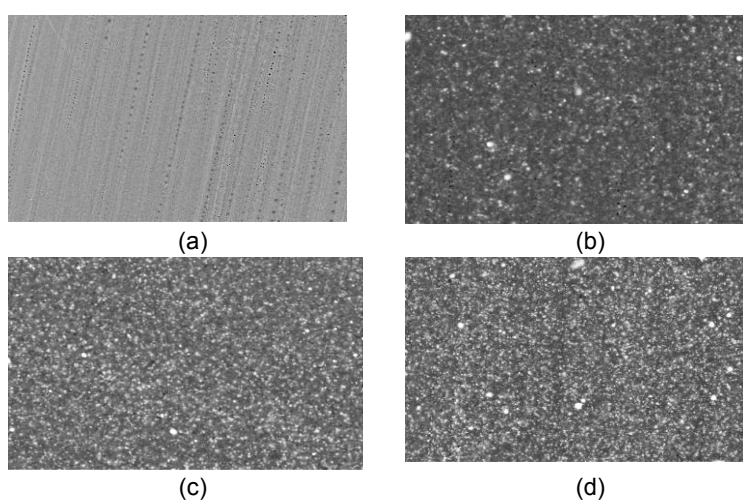

(a)

(b)

(c)

(d)

Figure 2: Surface micrograph of sample (a) A.1, (b) A.2, (c) A.3 and (d) A.4 under 1,000x magnification

SEM surface micrograph (Figure 2) revealed that white spots could be seen in all ZnO-NP containing samples (A.2-A.4) with larger amount of it in A.4 as compared to A.3 and A.2 samples. Similar micrographs have also been noted by other researchers that utilize ZnO-NP in their work (Balta et al., 2012). With the absence of this white spot in sample A.1 (without ZnO-NP), it is hypothesised that ZnO-NP has been successfully being incorporated into the membranes without any major agglomeration occurs. Nevertheless, it was noted that the extent of segregation of ZnO-NP and the verification of the white spot as ZnO-NP could not be measured quantitatively by solely using SEM micrograph. It is worth to note that the surface pores in A.1 are somehow line up along the length of the membrane, and presumably also occurs in other samples (could not be clearly seen due to white spots). It is suggested that this occurred due to the gravitational stretching during the air gap phase during the spinning. As the same effect was not seen on the white spot's dispersion, it is presumed that the phenomena were due to the addition of PVA.

3.2 Flux & Rejection Performance

Average pure water flux (PWF) of the HF membrane samples (Figure 3(a)) showed about 11.83 % increase in water flux from 37.72 $kg/m^2.h$ in A.1 sample to 42.18 $kg/m^2.h$ in A.2 sample. The increase in water flux suggested that HF membranes embedded with ZnO-NP were able to give improved flux performance as compared to the pristine membrane, as noted by several other researchers discussed earlier. The flux performances degraded by 5.98 % and 24.72 % for A.3 and A.4 samples as compared to the pristine A.1 sample, which corresponded to the PWF of 35.46 $kg/m^2.h$ and 28.40 $kg/m^2.h$. Similar results could also be noted for humid acid flux (HAF) which peaked out at 40.54 $kg/m^2.h$ for A.2 sample, followed by pristine A.1 at 36.02 $kg/m^2.h$, A.3 at 34.05 $kg/m^2.h$ and A.4 at 27.45 kg/m2.h. It is also worth noted that the improvement and degradation of HAF was at a similar level as for PWF, which was 12.56 % improvement for A.2 and flux degradation of 5.48 % and 23.78 % for A.3 and A.4.
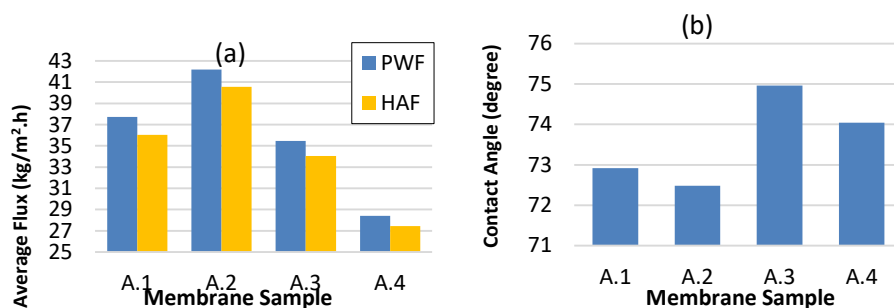
Figure 3: (a) Average fluxes (pure water flux, PWF and humic acid flux, HAF), (b) contact angle measurement of the membrane samples

This suggest that all membranes exhibit similar flux degradation in HA solution. The results for contact angles (CA) are presented in Figure 3(b), in which the lowest contact angle was noted for sample A.2 at 72.48°, followed by sample A.1 at 72.92°, sample A.4 at 74.04° and sample A.3 at 74.96°. There was an inverse trend exhibit by the contact angle measurement as compared to the average flux in Figure 3(a), which supported the trend of the flux. Contact angle is notable to be an indicator of the membrane's surface hydrophilicity, which is an indicator of membrane fouling behaviour (Tiraferri et al., 2012). Sample A.2, which exhibit the lowest CA showed the highest flux among the others, due to the increased hydrophilicity of the sample. The use of PVA at 1 wt% in sample A.1 showed comparable CA value with literature (Yuan et al., 2014). With the addition of 1 wt% of ZnO-NP in sample A.2, CA was able to be reduced even further. The changes in CA between the samples however were noted to be quite small. It is hypothesised that better hydrophilicity could be obtained by adjusting the ZnO-NP concentration between 0 wt% to 1 wt%, and by optimising the PVA concentration.

The graph of HAF vs time (Figure 4(a)) also showed an almost constant flux throughout the 2 h testing period. It is safe to assume that no major fouling happens for all the membrane samples. The HA rejection of the HF membrane samples (Figure 4(b)) showed significant improvement in rejection performances for ZnO-NP embedded membranes at 92.81 %, 94.43 % and 87.12 % for A.2, A.3 and A.4 samples as compared to 83.30 % noted for A.1 sample. All A.2, A.3 and A.4 sample improvements, which corresponds to 11.42 %, 13.36 % and 4.59 % increase in HA rejections suggested that the incorporation of ZnO-NP was beneficial towards improving the rejection of foulant in the solution. It is worth noted that the A.4 samples, albeit showed improvement over the pristine A.1, was still showing a decrease in rejection as compared to A.2 and A.3 samples. The rejection was inversely proportional to the flux of the membrane. Based on the flux and HA rejection performances, the incorporation of 1 wt% of ZnO-NP in A.2 sample showed that the embedded ZnO-NP was able to improve both the flux and rejection beyond the pristine A.1 sample. This suggest that ZnO-NP at low concentration was able to improve the hydrophilicity of the membranes. At the same time, the incorporation of ZnO-NP was also able to reduce the pore size of the membranes as noted by the literature (Ahmad et al., 2014). The addition of ZnO-NP increased the dope solution viscosity and produce membranes with smaller pore size. This in turns improved the rejection of the HA foulant for all ZnO-NP incorporated samples. While the reduction of flux between A.2 and A.3 samples could be explained through the inverse flux-rejection relations, the sudden decrease in rejection for A.4 samples as compared to A.3 was not expected. As HAF vs time graph in Figure 4(a) did not suggest any major fouling occurred, one hypothesis is that the incorporation of ZnO-NP at high concentration have lower suppression for macro pore formation, as noted in Figure 1. This in turns reduced the rejection percentage of HA. Nevertheless, it is too early for the hypothesis to be concluded and hence further test and characterisation should be done to verify the statements.
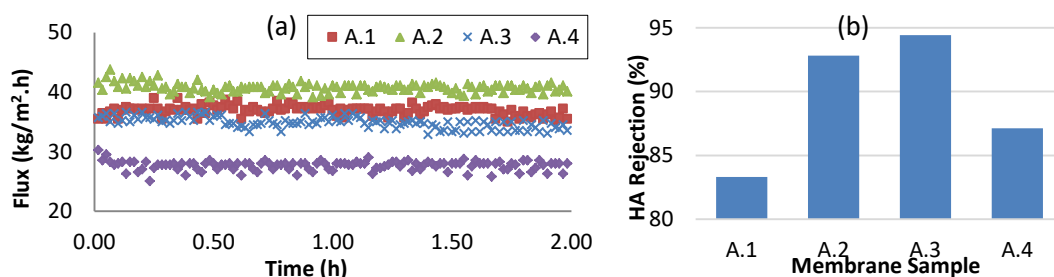

Figure 4: (a) HAF versus time on ZnO concentration, and (b) humic acid rejection with ZnO concentration

4. Conclusions

Nanocomposite hollow fibre membranes through blends of PVA, LiCl, PES, ZnO-NP and DMAc were successfully fabricated. Good dispersion of ZnO-NP can be noted visually through the SEM. Improvement in PWF was noted through 1 wt% addition of ZnO-NP, while improvement in HA rejection was noted in all ZnO-NP embedded HF membranes. ZnO-NP stabilised by PVA-LiCl mixture could be used as additive to improve the performance of PES based HF membranes. This preliminary study showed that HF membranes could be spun and be able to be self-supporting using the formula. The HF membranes are ready to be further tested and characterised for waste water treatment, particularly in antifouling application.

Acknowledgments

Reference

Ahmad A.L., Abdulkarim A.A., Ismail S., Ooi B.S., 2014, Preparation and characterisation of PES-ZnO mixed matrix membranes for humic acid removal, Desalination and Water Treatment 54, 3257-3268.

Balta S., Sotto A., Luis P., Benea L., Van Der Bruggen B., Kim J., 2012, A new outlook on membrane enhancement with nanoparticles, The alternative of ZnO, Journal of Membrane Science 389, 155-161.

Chetri P., Dass N.N., Sen Sarma N., 2008, Development of a catalyst for solution of poly(vinyl alcohol) in non-aqueous medium, Chinese Journal of Polymer Science 26, 399-404.

DROPimage Advanced, Ramé-hart Instrument co., New Jersey, United States.

Ghosh R., 2009, Ultrafiltration Based Protein Bioseparation, Handbook of Membrane Separations: Chemical, Pharmaceutical, Food and Biotechnological Applications, CRC Press, Florida, USA.

Guillen G.R., Pan Y., Li M., Hoek E.M.V., 2011, Preparation and Characterization of Membranes Formed by Nonsolvent Induced Phase Separation: A Review, Industrial and Engineering Chemistry Research 50, 3798-3817.

Moch Jr.I., 2004, Hollow Fiber Membranes, Encyclopedia of Desalination and Water Resources (DESWARE), Eolss Publishers Co. Ltd., Paris, France.

Kirk-Othmer, 1998, Hollow Fiber Membranes, Kirk-Othmer Encyclopedia of Chemical Technology Vol 13, Ed. Kirk-Othmer, John Wiley & Sons Inc, New Jersey, United States.

Leo C.P., Cathie Lee W.P., Ahmad A.L., Mohammad A.W., 2012, Polysulfone membranes blended with ZnO nanoparticles for reducing fouling by oleic acid, Separation and Purification Technology 89 , 51-56.

Li N., Xiao C., An S., Hu X., 2010, Preparation and properties of PVDF/PVA hollow fiber membranes, Desalination 250, 530-537.

Ng L.Y., Leo C.P., Mohammad A.W., 2011, Optimizing the incorporation of silica nanoparticles in polysulfone/poly(vinyl alcohol) membranes with response surface methodology, Journal of Applied Polymer Science 121, 1804-1814.

Tiraferri A., Kang Y., Giannelis E.P., Elimelech M., 2012, Superhydrophilic thin-film composite forward osmosis membranes for organic fouling control: fouling behavior and antifouling mechanisms, Environmental Science & Technology 46, 11135-11144.

Tosh B., Saikia C.N., Dass N.N., 1999, Development of a nonaqueous solvent system for poly(vinyl alcohol) and its characterization, Journal of Applied Polymer Science 74, 663-669.

Ulbricht M., 2011, Porous Flat Sheet, Hollow Fibre and Capsule Membranes by Phase Separation of Polymer Solutions, Eds. Basile A., Gallucci F, Membranes for Membrane Reactors: Preparation, Optimization and Selection. John Wiley and Sons Ltd, New Jersey, United States.

Yuan H., Wang Y., Cheng L., Liu W., Ren J., Meng L., 2014, Improved Antifouling Property of Poly(ether sulfone) Ultrafiltration Membrane through Blending with Poly(vinyl alcohol), Industrial and Engineering Chemistry Research 53, 18549-18557.

Zhang J., Wang Q., Wang Z., Zhu C., Wu Z., 2014, Modification of poly(vinylidene fluoride)/polyethersulfone blend membrane with polyvinyl alcohol for improving antifouling ability, Journal of Membrane Science 466, 293-301.

Zhao S., Yan W., Shi M., Wang Z., Wang J., Wang S., 2015, Improving permeability and antifouling performance of polyethersulfone ultrafiltration membrane by incorporation of ZnO-DMF dispersion containing nano-ZnO and polyvinylpyrrolidone, Journal of Membrane Science 478, 105-116.